

# A Cell Capacitor Energy Balancing Control of MMC-HVDC under the AC Grid Faults

Jae-Jung Jung<sup>1</sup>, Shenghui Cui<sup>2</sup>, Younggi Lee<sup>1</sup>, and Seung-Ki Sul<sup>1</sup>

<sup>1</sup> Seoul National University, Seoul, Korea

<sup>2</sup> E.ON Energy Research Center, RWTH Aachen University, Germany

**Abstract--** This paper presents the techniques for regulation of system balancing in modular multilevel converter (MMC) based HVDC system under the AC grid double line fault condition. Due to the special structure of MMC, the balancing of the cell capacitor voltage is crucial for any operating circumstance of the system. Also, the responses against the grid faults of HVDC system based on MMC are different to those based on the conventional voltage sourced converters. Therefore, even under the non-permanent fault in AC grid, the balancing of the cell capacitor energy of MMC has to be guaranteed continuously. Among AC grid fault modes, the double line fault causes one of the most severe transients in MMC. In this paper, a balancing control method of MMC based on an offset voltage injection strategy in the output reference voltages is proposed. By the virtue of the proposed method, the HVDC system based on MMC can have the enhanced fault ride-through capability against the double line fault in AC grid. The validity of the proposed method is verified by simulation results of a ±200kV, 400MVA point-to-point HVDC system.

**Index Terms—** AC grid fault, arm energy balancing, double line fault, modular multilevel converter, voltage source converter based HVDC

## I. INTRODUCTION

Voltage Source Converter (VSC) for High Voltage Direct Current (HVDC) transmission is a promising solution for the future smart grid which would integrate a great amount of renewable energy sources into the existing AC grid. Compared to the Line Commutated Converter (LCC) based HVDC, VSC-HVDC has the advantages such as black start capability, active/reactive power control, and power supply for weak AC grid. For VSC-HVDC, especially, a Modular Multilevel Converter (MMC) is a competitive candidate and is attracting worldwide attention [1-3]. MMC presents many advantages such as very low harmonics, low dv/dt, modularity and simple scaling, high reliability and low switching loss, no necessity of series connection of power semiconductors, and the DC bus capacitor elimination [4-6], etc. One of major concerns in HVDC transmission systems is about faults and many studies had been done in depth [7-8, 10]. According to the duration of the faults, they can be divided into permanent and non-permanent faults. The permanent fault affects the system functional behavior permanently and they are also referred to as solid or hard faults. Generally, the non-permanent fault affects the system functional behavior only part of the time. And, the system controller could have fault ride-through capability and the system operates normally

without any trip even under the faults. Among these faults in AC grid, the single line-to-ground (SLG) fault is the dominant fault mode in the practical transmission line. Therefore, the countermeasures against SLG faults had been investigated in many articles especially with regard to HVDC system based on MMC (MMC-HVDC). To deal with the unbalanced grid conditions, a Double Synchronous Reference Frame (DSRF) current control scheme including positive- and negative-sequence current controller based on vector control concept was introduced in [11], and applied to two-level and three-level grid connected VSCs. This control scheme had been also applied to the control of MMC- HVDC. Meanwhile, in [13] for reducing time delay caused by notch filters in DSRF controller of [11], the AC grid current references including both positive- and negative-sequence components were transformed to the stationary reference frame. To guarantee the zero steady state error, the Proportional and Resonance (PR) controllers were employed. At the asymmetric faults where negative sequence component arise, it is general to eliminate the negative-sequence currents for maintaining symmetric grid currents. This paper can be considered as an extension of works done in [9-10]. In [9], the positive- and negative-sequence circulating current was used to balance the MMC system. However, Ref. [9] has no consideration about the negative-sequence output voltage produced by the grid current controller and it only used the positive-sequence of the AC output voltages. Because the negative-sequence output voltage makes uncontrolled counterbalancing power terms, Ref. [10] proposed a method that the positive- and negative-sequence circulating currents were recalculated considering unbalanced grid conditions. Even in [10], however, when the magnitudes of positive- and negative-sequence output voltage are almost equal in case of double line faults, the solutions of the circulating current references would not exist. In this paper, against the double line fault the offset voltage is introduced for the balancing controller of the MMC system, which is fully decoupled from the power flow controllers. Therefore, the proposed fault ride through method can improve the dynamic performances of MMC under the severe grid fault condition, especially double line grid fault. When double line fault occurs, the controller starts injecting offset voltage and achieves the balance of an MMC during the fault period. By the virtue of the proposed method the fault ride-through capability of the MMC-HVDC system can be enhanced conspicuously. To verify the validity of the conducted work in this paper, computer simulations by PSIM are

performed by a full scale simulation model,  $\pm 200\text{kV}$ ,  $400\text{MVA}$  point-to-point HVDC system (216 sub-modules per arm).

## II. CONFIGURATION AND BASIC PRINCIPLE OF THE MMC

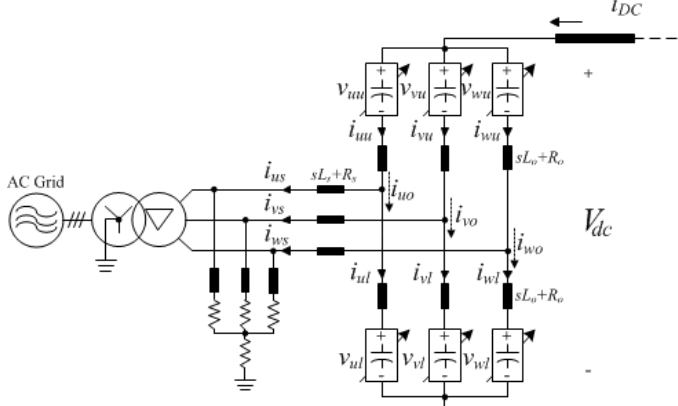


Fig. 1. Simplified schematic of an MMC in HVDC application.

The simplified circuit configuration of an MMC in HVDC application under study is shown in Fig. 1. An MMC consists of three legs for three phases, and each leg has two arms, respectively the upper and the lower arm. An arm usually consists of numerous half- or full-bridge based sub-modules called as cells and the whole arm can be modeled as a high bandwidth controlled voltage source with a capacitor tank. The AC side of MMC is connected to AC grid through a Y/ $\Delta$  transformer for preventing the zero-sequence phase currents from flowing into the converter. The MMC is typically grounded through the AC side by a star point reactor grounding device or a zig-zag transformer grounding device [15]. For detailed mathematical description of the model of MMC, the equivalent circuit diagram can be derived as Fig. 2 [9-10]. In Fig. 2,  $i_{xu}$  and  $i_{xl}$  stand for upper and lower arm currents, respectively, and  $i_{xs}$  for the grid current, where ‘ $x$ ’ denotes a phase among  $u$ ,  $v$ , and  $w$ . In accordance with the conventional definitions, the upper and lower arm, the leg and the circulating current can be defined and deduced as (1)-(4), respectively.

$$i_{xu} = \frac{1}{2}i_{xs} + i_{xo} . \quad (1)$$

$$i_{xl} = -\frac{1}{2}i_{xs} + i_{xo} . \quad (2)$$

$$i_{xo} = \frac{i_{xu} + i_{xl}}{2} = i_{xo,cir} + \frac{1}{3}i_{DC} . \quad (3)$$

$$i_{xo,cir} = i_{xo,cirDC} + i_{xo,cirAC} . \quad (4)$$

The phase voltage  $v_{xs}$  can be used to regulate the grid current and the leg current  $i_{xo}$  can be regulated by the leg internal voltage  $v_{xo}$ . The phase and leg internal voltage are defined as (5) and (6), respectively.

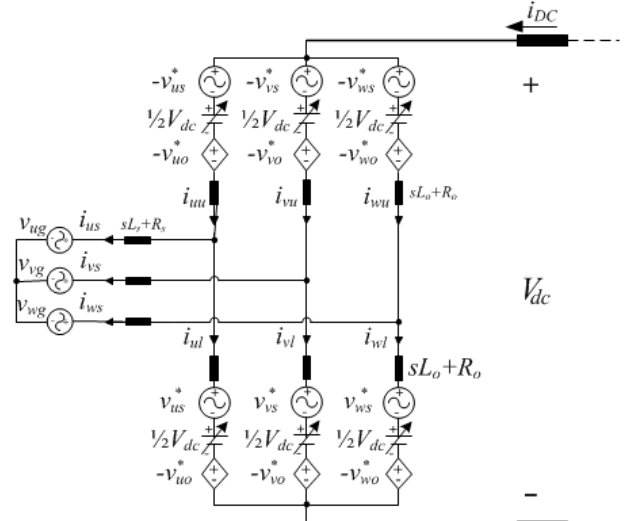


Fig. 2. Equivalent circuit diagram of the MMC.

$$v_{xs} = -\frac{1}{2}(v_{xu} - v_{xl}) . \quad (5)$$

$$v_{xo} = \frac{1}{2}\{V_{dc} - (v_{xu} + v_{xl})\} = \left(R_o + L_o \frac{d}{dt}\right)i_{xo} . \quad (6)$$

Therefore, the upper and lower arm voltage reference should be (7) and (8) for the desired performances of MMC. Namely, the arm voltage references are sum of independent components for regulating DC bus current, AC output current, and leg current.

$$v_{xu}^* = \frac{V_{dc}^*}{2} - v_{xs}^* - v_{xo}^* . \quad (7)$$

$$v_{xl}^* = \frac{V_{dc}^*}{2} + v_{xs}^* - v_{xo}^* . \quad (8)$$

From the above descriptions, the control strategy of the capacitor energy in MMC can be deduced. Both DC bus voltage and AC power reference should be determined to keep the total capacitor energy in MMC. Therefore, the controllable component of circulating current has to be used to balance the capacitor energy among six arms. To balance the arm capacitor energy, the power flow in a leg should be considered. Power that flows into upper and lower arms in the same leg are:

$$P_{xu} = v_{xu}^* i_{xu} = \left(\frac{V_{dc}^*}{2} - v_{xs}^* - v_{xo}^*\right)\left(\frac{1}{2}i_{xs} + i_{xo}\right) . \quad (9)$$

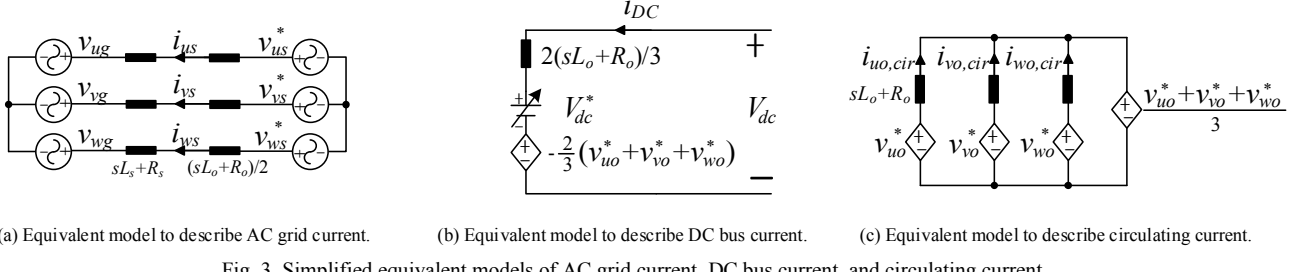
$$P_{xl} = v_{xl}^* i_{xl} = \left(\frac{V_{dc}^*}{2} + v_{xs}^* - v_{xo}^*\right)\left(-\frac{1}{2}i_{xs} + i_{xo}\right) . \quad (10)$$

Then, the sum and difference of the power between upper and lower arms are:

$$P_{legx}^\Sigma = P_{xu} + P_{xl} = V_{dc}^* i_{xo} - v_{xs}^* i_{xs} - 2v_{xo}^* i_{xo} . \quad (11)$$

$$P_{legx}^\Delta = P_{xu} - P_{xl} = \frac{1}{2}V_{dc}^* i_{xs} - 2v_{xs}^* i_{xo} - v_{xo}^* i_{xs} . \quad (12)$$

And these two equations have to be considered for the understanding of the subsequent proposed balancing control. The sum of upper and lower arm energy,  $E_x^\Sigma$ , should be controlled by the first power term in right side of (11). Thus, a DC component of leg current,  $i_{xo}$ , is injected to regulate  $E_x^\Sigma$ . The difference of upper and



(a) Equivalent model to describe AC grid current.

(b) Equivalent model to describe DC bus current.

(c) Equivalent model to describe circulating current.

lower arm energy,  $E_x^\Delta$ , should be counterbalanced by the second term in right side of (12). So, a fundamental frequency component of leg current  $i_{xo}$  is injected to control  $E_x^\Delta$ .

### III. MMC MODELING IN VSC-HVDC TRANSMISSION

In [11], a new equivalent model of MMC for energy control of cell capacitor had been presented, which divided the MMC model like Fig. 2 into AC grid current model, DC bus current model, and circulating current model. According to the equivalent model of MMC, the AC grid power control and DC bus voltage control can be decoupled.

The equivalent circuit diagram in Fig. 2 can be divided into three aforementioned simplified equivalent models like Fig. 3. First, for phases ‘ $x$ ’ and ‘ $y$ ’, according to KVL, the transient response of upper and lower arm currents can be derived as (13) and (14).

$$\begin{aligned} & -v_{xs}^* + \frac{1}{2}V_{dc}^* - v_{xo}^* + (L_o \frac{d}{dt} + R_o)i_{xu} + (L_s \frac{d}{dt} + R_s)i_{xs} + v_{xg} \\ &= -v_{ys}^* + \frac{1}{2}V_{dc}^* - v_{yo}^* + (L_o \frac{d}{dt} + R_o)i_{yu} + (L_s \frac{d}{dt} + R_s)i_{ys} + v_{yg}. \end{aligned} \quad (13)$$

$$\begin{aligned} & v_{xs}^* + \frac{1}{2}V_{dc}^* - v_{xo}^* + (L_o \frac{d}{dt} + R_o)i_{xl} - (L_s \frac{d}{dt} + R_s)i_{xs} - v_{xg} \\ &= v_{ys}^* + \frac{1}{2}V_{dc}^* - v_{yo}^* + (L_o \frac{d}{dt} + R_o)i_{yl} - (L_s \frac{d}{dt} + R_s)i_{ys} - v_{yg}. \end{aligned} \quad (14)$$

Both of (13) and (14) can be expressed as (15) which is a basis of AC grid current model, using the definition of leg current in (3) and leg internal voltage in (6).

$$\begin{aligned} & v_{xs}^* - (L_o \frac{d}{dt} + R_o)i_{xs} / 2 - (L_s \frac{d}{dt} + R_s)i_{xs} - v_{xg} \\ &= v_{ys}^* - (L_o \frac{d}{dt} + R_o)i_{ys} / 2 - (L_s \frac{d}{dt} + R_s)i_{ys} - v_{yg}. \end{aligned} \quad (15)$$

According to (15), a simplified equivalent model to describe the AC grid current can be extracted from Fig. 2, as shown in Fig. 3(a).

Second, the instantaneous DC bus voltage equations of  $u$ -,  $v$ -, and  $w$ -phase by KVL for Fig. 2 can be described as (16).

$$\begin{cases} (-v_{us}^* + \frac{V_{dc}^*}{2} - v_{uo}^*) + (L_o \frac{d}{dt} + R_o)(i_{uu} + i_{ul}) + (v_{us}^* + \frac{V_{dc}^*}{2} - v_{uo}^*) = V_{dc} \\ (-v_{vs}^* + \frac{V_{dc}^*}{2} - v_{vo}^*) + (L_o \frac{d}{dt} + R_o)(i_{vu} + i_{vl}) + (v_{vs}^* + \frac{V_{dc}^*}{2} - v_{vo}^*) = V_{dc} \\ (-v_{ws}^* + \frac{V_{dc}^*}{2} - v_{wo}^*) + (L_o \frac{d}{dt} + R_o)(i_{wu} + i_{wl}) + (v_{ws}^* + \frac{V_{dc}^*}{2} - v_{wo}^*) = V_{dc} \end{cases} \quad (16)$$

After summation of three equations in (16), DC bus voltage can be deduced as (17).

$$V_{dc}^* + \frac{2}{3}(L_o \frac{d}{dt} + R_o)i_{dc} - \frac{2}{3}(v_{uo}^* + v_{vo}^* + v_{wo}^*) = V_{dc}. \quad (17)$$

According to (17), a simplified equivalent model to describe the DC bus current can be extracted from Fig. 2, as shown in Fig. 3(b).

Meanwhile, (18) can be derived after canceling an  $x$ -phase equation of (16) and (17) by the DC bus voltage,  $V_{dc}$ .

$$(L_o \frac{d}{dt} + R_o)(i_{xo} - \frac{i_{dc}}{3}) = v_{xo}^* - \frac{v_{uo}^* + v_{vo}^* + v_{wo}^*}{3}. \quad (18)$$

A circulating current  $i_{xo,cir}$  is defined as the difference between the leg current  $i_{xo}$  and a third of the DC bus current that identically flows into each phase:

$$i_{xo,cir} = i_{xo} - \frac{i_{dc}}{3}. \quad (19)$$

Therefore, (20) can be derived from (18) and (19).

$$v_{xo}^* - (L_o \frac{d}{dt} + R_o)i_{xo,cir} = \frac{v_{uo}^* + v_{vo}^* + v_{wo}^*}{3}. \quad (20)$$

And finally, according to (20), a simplified equivalent model to describe the circulating current can be extracted from Fig. 2, as shown in Fig. 3(c). For a three phase MMC, sum of three phase leg currents is equal to the DC bus current. Then, a basic characteristic of the circulating current can be deduced as (21).

$$i_{uo,cir} + i_{vo,cir} + i_{wo,cir} = 0. \quad (21)$$

Eq. (21) means that the circulating currents only flow inside the converter without being leaked to neither the AC grid side nor the DC bus side.

The average of three phase leg internal voltages ( $v_{uo}^*$ ,  $v_{vo}^*$ ,  $v_{wo}^*$ ) is defined as (22) which is the common mode leg internal voltage  $v_{o,com}^*$ .

$$v_{o,com}^* = \frac{v_{uo}^* + v_{vo}^* + v_{wo}^*}{3}. \quad (22)$$

As shown in Fig. 3(b), the common mode leg internal voltage  $v_{o,com}^*$  affects the real DC bus voltage  $V_{dc}$ .

Furthermore,  $v_{o,com}^*$  of the circulating current model also affects circulating currents as shown in Fig. 3(c). So, in the case of weak DC bus condition in HVDC transmission system, the control dynamics and system performance would significantly depend on the common mode leg internal voltage  $v_{o,com}^*$ . And,  $v_{o,com}^*$  should be

controlled as null. Based on above MMC modeling, which can completely decouple AC current regulation, DC current regulation, and cell capacitor energy control, at section IV the capacitor energy balancing strategies under balanced and unbalanced grid conditions are derived.

#### IV. BALANCING CONTROL UNDER AC GRID DOUBLE LINE FAULT CONDITION

##### A. Vector Controller of AC Grid Current for Unbalanced AC Grid Conditions

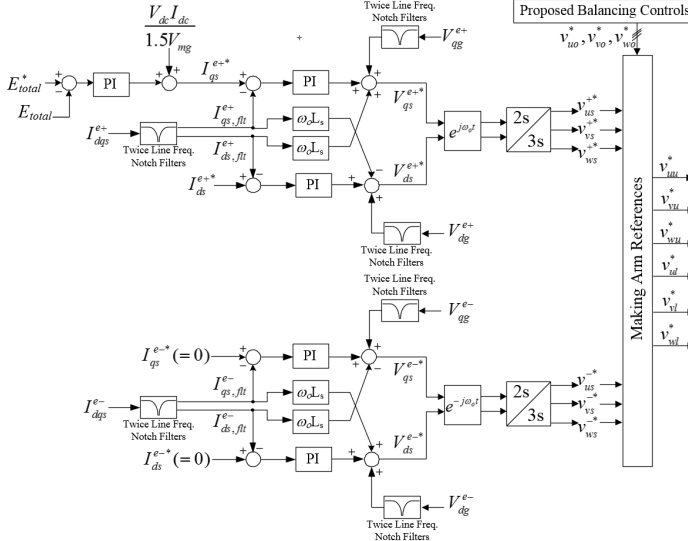


Fig. 4. Schematic of a vector controller of AC grid current for unbalanced grid conditions.

When the unbalanced grid faults occur, one of the requirements to the faults is balancing of the grid currents. And, the negative-sequence currents in grid should be controlled as null even in the faults. This could minimize the fault current that may make detrimental effects on the converter. In such situation, the positive sequence AC grid current and the negative sequence AC grid current should be controlled independently, and it calls for two independent AC grid current vector controllers, namely a positive sequence AC grid current controller and a negative sequence AC grid current controller. Fig. 4 shows the control block diagram of the vector controller of AC grid current for unbalanced grid conditions [14]. Therefore, the positive sequence grid current controller only generates reference of the positive sequence output EMF, and the negative sequence grid current controller only generates reference of the negative sequence output EMF. As discussed in Section III, control of the DC bus current and the circulating current are not affected by AC grid side by the proposed method, no matter the AC grid is balanced or not. It is shown in (11) that the output EMF does not contribute to the power associated with the leg capacitor energy balancing. However, since upper and lower arm capacitor energy control strategy proposed in (12) is conducted under an assumption of balanced AC grid, unbalanced AC grid faults would result in

disturbance power that associated with upper and lower arm capacitor energy balancing control. Meanwhile, as shown like Fig. 1, Y/D transformer connected to AC grid excludes the argument about the zero-sequence component from the converter.

##### B. Three Phase Leg Energy Balancing Control

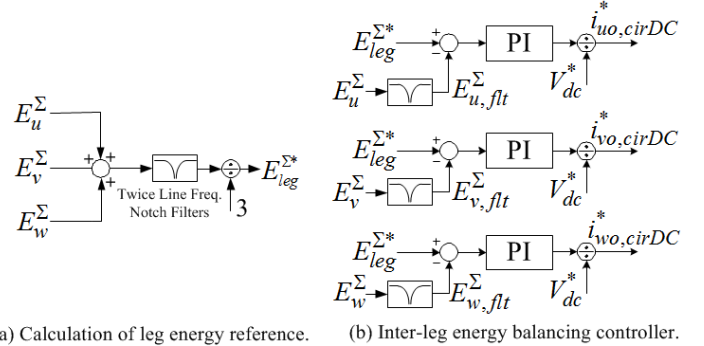


Fig. 5. Control block diagram of the proposed leg capacitor energy balancing controller.

The circulating current defined in (19) that flows only inside the converter can transfer energy between different arms without affecting neither AC grid current nor DC bus current. And, it is employed in the proposed control strategy for arm capacitor energy balancing. The power flow into three different legs expressed in (11) and (19) can also be represented as (23).

$$P_{legx}^{\Sigma} = \frac{dE_x^{\Sigma}}{dt} = \left( V_{dc}^* \frac{i_{dc}}{3} - V_{xs}^* i_{xs} \right) + V_{dc}^* i_{xo,cir}. \quad (23)$$

The terms in parenthesis of the right hand side of (23) are determined by power flow and the converter total capacitor energy controller. In the steady state, the terms would be cancelled if the AC grid is balanced. Since the sum of the circulating currents is inherently null as (21), if a DC component is injected in the circulating currents, three-phase sum of the last term in the right hand sides of (23) is inherently null as (24).

$$V_{dc}^* i_{uo,cirDC} + V_{dc}^* i_{vo,cirDC} + V_{dc}^* i_{wo,cirDC} = 0. \quad (24)$$

The control block diagram of the proposed leg capacitor energy balancing controller is shown in Fig. 5. The leg capacitor energy reference is updated as the average capacitor energy of three phase legs at every sampling instant as shown in Fig. 5(a). The philosophy of using the average energy of three legs as the reference is balancing the leg capacitor energy by only regulating the DC components of the circulating currents as shown by the outputs of controllers in Fig. 5(b). Because the leg capacitor energy reference is calculated and updated at every sampling period, it can be valid that the common mode leg internal voltage  $v_{o,com}^*$  is inherently null, as (25).

$$\begin{aligned} \sum_{x=u,v,w} (E_{leg}^{\Sigma*} - E_{x,flt}^{\Sigma}) &= 0. \\ \Rightarrow \sum_{x=u,v,w} i_{xo,cirDC}^* &= 0. \Rightarrow \sum_{x=u,v,w} v_{xo,DC}^* = 0. \end{aligned} \quad (25)$$

### C. Balancing of Upper and Lower Arm Capacitor Energy under Balanced Grid Conditions

Difference of power that flow into upper and lower arms can be derived as (26) from (12) and (19), and the last term of (12) has almost negligible effect on the energy balancing.

$$P_{\text{legx}}^{\Delta} = \frac{1}{2} V_{dc}^* i_{xs} - 2V_{xs}^* \frac{i_{dc}}{3} - 2V_{xs}^* i_{xo,cir}. \quad (26)$$

Since the first two terms in the right hand sides of (26) do not generate DC components, only the last term of the right hand sides can make a counterbalancing DC power component. Since the upper and lower arm capacitor energy should be balanced for three legs independently, three degree of freedoms (DOFs) are necessary to regulate  $P_x^{\Delta}$  ( $P_u^{\Delta}$ ,  $P_v^{\Delta}$ ,  $P_w^{\Delta}$ ) independently. In [9], positive and negative sequence circulating currents were employed. The three phase output EMFs are defined as (27).

$$\begin{cases} v_{us}^* = V_{ms} \cos(\omega_o t + \phi_v) \\ v_{vs}^* = V_{ms} \cos(\omega_o t + \phi_v - 2\pi/3) \\ v_{ws}^* = V_{ms} \cos(\omega_o t + \phi_v + 2\pi/3) \end{cases} \quad (27)$$

If a positive sequence circulating current is injected as (28) inside the MMC, the differences of power flow into upper and lower arm capacitors caused by the injected positive sequence circulating current can be deduced as (29), according to (26).

$$\begin{cases} i_{uo,cirAC}^{+*} = I_{cirAC}^+ \sin(\omega_o t + \phi_i^+) \\ i_{vo,cirAC}^{+*} = I_{cirAC}^+ \sin(\omega_o t + \phi_i^+ - 2\pi/3) \\ i_{wo,cirAC}^{+*} = I_{cirAC}^+ \sin(\omega_o t + \phi_i^+ + 2\pi/3) \end{cases} \quad (28)$$

$$\begin{cases} P_u^{+\Delta} = -V_{ms} I_{cirAC}^+ \cos(\phi_v - \phi_i^+) \\ P_v^{+\Delta} = -V_{ms} I_{cirAC}^+ \cos(\phi_v - \phi_i^+) \\ P_w^{+\Delta} = -V_{ms} I_{cirAC}^+ \cos(\phi_v - \phi_i^+) \end{cases} \quad (29)$$

In (29), the injected positive sequence circulating current only contributes to common components of  $P_x^{\Delta}$ ,

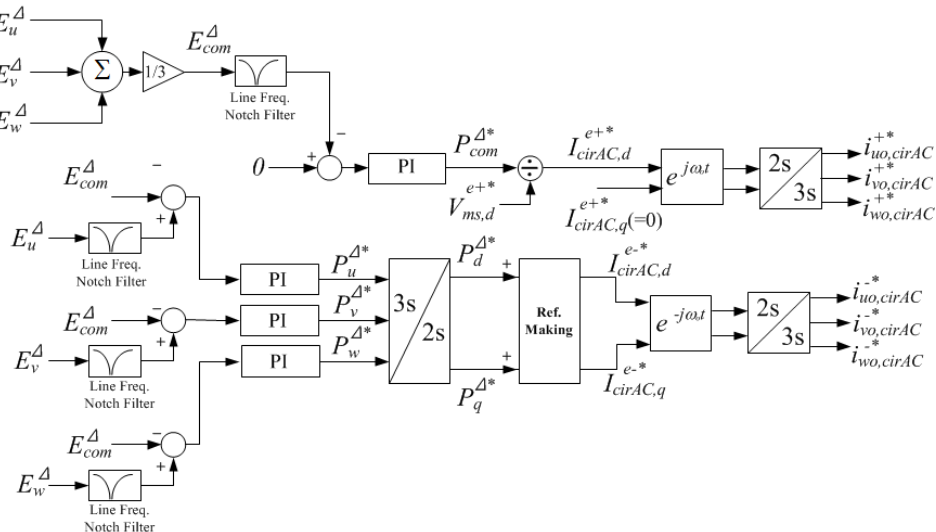


Fig. 6. Schematic of proposed arm energy balancing method under balanced grid conditions.

which means that it can be injected to eliminate only common errors of upper and lower arm capacitor energy of three phases in an MMC.

If a negative sequence circulating current is injected inside the MMC as (30), then according to (26), differences of power that flow into upper and lower arm capacitors caused by the injected negative sequence circulating current can be deduced as (31).

$$\begin{cases} i_{uo,cirAC}^{-*} = I_{cirAC}^- \sin(\omega_o t + \phi_i^-) \\ i_{vo,cirAC}^{-*} = I_{cirAC}^- \sin(\omega_o t + \phi_i^- + 2\pi/3) \\ i_{wo,cirAC}^{-*} = I_{cirAC}^- \sin(\omega_o t + \phi_i^- - 2\pi/3) \end{cases} \quad (30)$$

$$\begin{cases} P_u^{-\Delta} = -V_{ms} I_{cirAC}^- \cos(-\phi_v + \phi_i^-) \\ P_v^{-\Delta} = -V_{ms} I_{cirAC}^- \cos(-\phi_v + \phi_i^- - 2\pi/3) \\ P_w^{-\Delta} = -V_{ms} I_{cirAC}^- \cos(-\phi_v + \phi_i^- + 2\pi/3) \end{cases} \quad (31)$$

In (31), the injected negative sequence circulating current only contributes to differential components of  $P_x^{\Delta}$ , which means that it can be injected to eliminate only differential errors of upper and lower arm capacitor energy of three phases in an MMC.

Therefore, the positive and negative sequence circulating current can be injected to eliminate both common and differential errors of upper and lower arm capacitor energy of three phases. In (29) and (31), if the injected positive sequence circulating current is in phase with the output EMF, namely  $\phi_v = \phi_i^+$ , then  $I_{cirAC}^+$ ,  $I_{cirAC}^-$ ,  $\phi_i^+$  provides three DOFs for upper and lower arm capacitor energy balancing. Then the positive sequence circulating current can be injected to eliminate the common error  $E_{com}^{\Delta}$  of upper and lower arm capacitor energy, and the negative sequence circulating current can be injected to eliminate the differential error  $E_d^{\Delta}$  and  $E_q^{\Delta}$  of upper and lower arm capacitor energy as deduced by (32).

$$\begin{cases} P_{com}^{\Delta} = \frac{dE_{com}^{\Delta}}{dt} = \frac{d}{dt}\left\{\frac{1}{3}(E_u^{\Delta} + E_v^{\Delta} + E_w^{\Delta})\right\} = -V_{ms}I_{cirAC}^{+} \\ P_d^{\Delta} = \frac{dE_d^{\Delta}}{dt} = \frac{d}{dt}\left(\frac{2}{3}E_u^{\Delta} - \frac{1}{3}E_v^{\Delta} - \frac{1}{3}E_w^{\Delta}\right) = -V_{ms}I_{cirAC}^{-} \cos(\phi_i^- - \phi_v) \\ P_q^{\Delta} = \frac{dE_q^{\Delta}}{dt} = \frac{d}{dt}\left(\frac{\sqrt{3}}{3}E_v^{\Delta} - \frac{\sqrt{3}}{3}E_w^{\Delta}\right) = -V_{ms}I_{cirAC}^{+} \sin(\phi_i^- - \phi_v) \end{cases}. \quad (32)$$

Since for upper and lower arm capacitor energy balancing references of line frequency component circulating currents only include positive and negative sequence components, inherent nullification of common mode component of leg internal voltages is guaranteed as (33).

$$\sum_{x=u,v,w} v_{xo,AC}^* = 0 \Rightarrow \sum_{x=u,v,w} i_{xo,cirAC}^* = 0. \quad (33)$$

Control block diagram of the upper and lower arm capacitor energy balancing controller is shown in Fig. 6. Eq. (34) is used in the reference making block in Fig. 6 to make the reference of the negative sequence circulating current.

$$i_{cirAC,d}^{-*} + j i_{cirAC,q}^{-*} = \frac{P_d^{\Delta*} + j P_q^{\Delta*}}{-V_{ms}} e^{j(\omega_o t + \phi_v)}. \quad (34)$$

#### D. Balancing of Upper and Lower Arm Capacitor Energy under Unbalanced Grid Conditions

This paper proposes the capacitor energy balancing control method that can be applied under double line grid fault by using the switchover of balancing controller, as shown like Fig. 7. The basic principle of the balancing capacitor energy in the proposed method is the same as that in [9] which decouples the AC power control from the DC bus voltage control. And, in [9-10], the positive-sequence and negative-sequence circulating current were employed for cell capacitor energy balancing and for decoupling the AC and DC side of converter as described in case of the balanced grid conditions. Especially, in [10], a control strategy of the MMC for capacitor energy balancing had been presented, which was universally valid under both balanced and unbalanced grid condition

without any transition in control modes. Unfortunately, the method in [10] reveals a singular point in the case of double line grid fault where there is no solution of circulating current reference because the magnitudes of positive- and negative-sequence output voltages are the same.

Considering the grid fault conditions, the output phase voltage reference has the negative sequence components which should be generated inevitably to eliminate the negative grid currents as referred at Fig. 4. First, assuming unbalanced grid condition, the positive- and negative-sequence component of the output phase voltages are defined by (35) and (36), respectively.

$$\begin{cases} v_{us}^{+*} = V_{ms}^+ \sin(\omega_o t + \phi_v^+) \\ v_{vs}^{+*} = V_{ms}^+ \sin(\omega_o t + \phi_v^+ - 2\pi/3) \\ v_{ws}^{+*} = V_{ms}^+ \sin(\omega_o t + \phi_v^+ + 2\pi/3) \end{cases}. \quad (35)$$

$$\begin{cases} v_{us}^{-*} = V_{ms}^- \sin(\omega_o t + \phi_v^-) \\ v_{vs}^{-*} = V_{ms}^- \sin(\omega_o t + \phi_v^- + 2\pi/3) \\ v_{ws}^{-*} = V_{ms}^- \sin(\omega_o t + \phi_v^- - 2\pi/3) \end{cases}. \quad (36)$$

In this paper, the offset voltage in the arm references during double line fault is introduced. Under the fault situation, the circulating current has the two components which are the same frequency component with the injected offset voltage and the positive-sequence component. The negative-sequence component is excluded from the circulating current for balancing. The positive-sequence components contribute to counterbalancing of the upper and lower arm energy of three phases,  $E_{com}^{\Delta}$  in (37) which is the same as that in (32). For simplifying (32), the d-axis is oriented as the axis where all positive sequence phase voltage lies ( $V_{ms,q}^{e+} = 0$ ) and the q-axis component of positive sequence circulating current is controlled as null ( $I_{cirAC,q}^{e+} = 0$ ) in accordance with the aforementioned synchronization of  $\phi_v^+ = \phi_i^+$ . Likewise, the same frequency components with the offset voltage eliminate

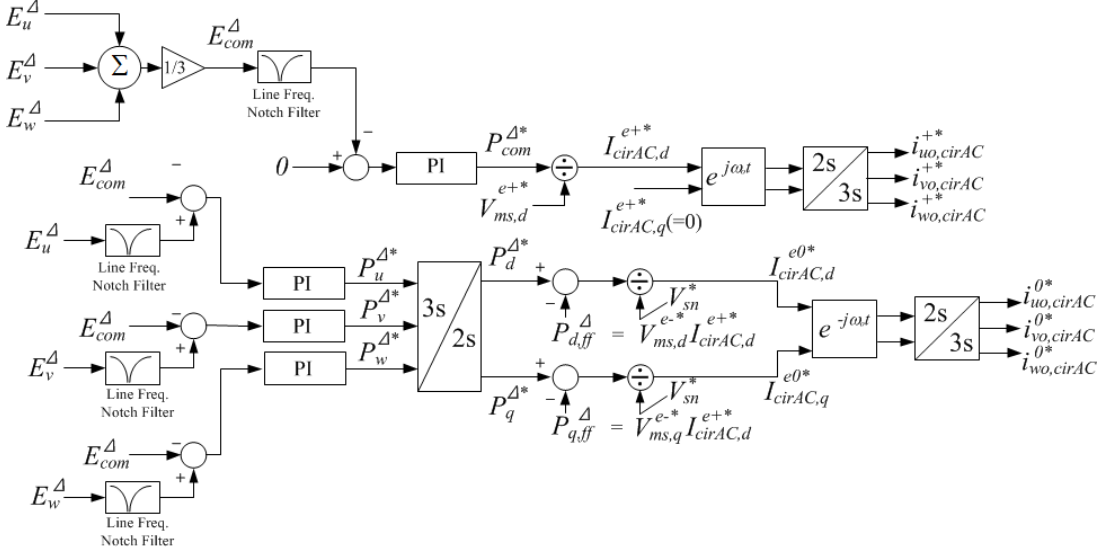


Fig. 7. Schematic of proposed arm energy balancing method under the AC double line faults.

three phase upper and lower arm capacitor energy differences,  $E_d^\Delta$  and  $E_q^\Delta$ . In (36) and (37), the power terms occurred by the product of negative-sequence output voltage and positive-sequence circulating current are notable. The positive-sequence circulating current for nullifying  $E_{com}^\Delta$  disturbs the upper and lower arm capacitor energy balancing. Therefore, this unintended power term should be considered and compensated by additional feedforward term as shown in Fig. 7. Under the double line grid faults, which are double line-to-ground and line-to-line fault, the power term made by the product of injected offset voltage and circulating current,  $I_{xo,cirAC}^{0*}$  with the same frequency plays a crucial role in upper and lower arm balancing.

$$\left\{ \begin{array}{l} P_{com}^\Delta = \frac{dE_{com}^\Delta}{dt} = \frac{d}{dt} \left\{ \frac{1}{3} (E_u^\Delta + E_v^\Delta + E_w^\Delta) \right\} = -V_{ms,d}^{e+} I_{cirAC,d}^{e+} \\ P_d^\Delta = \frac{dE_d^\Delta}{dt} = -V_{ms,d}^{e-} I_{cirAC,d}^{e+} + V_{sn}^* I_{cirAC,d}^{e0*} \\ P_q^\Delta = \frac{dE_q^\Delta}{dt} = -V_{ms,q}^{e-} I_{cirAC,d}^{e+} + V_{sn}^* I_{cirAC,q}^{e0*} \end{array} \right. . \quad (37)$$

## V. FULL SCALE SIMULATION STUDIES

A 400MVA full-scale version point-to-point MMC-HVDC transmission system is simulated by PSIM software, and the schematic of the system is shown in Fig. 8. The parameters for the computer simulation are listed in Table I.

TABLE I  
PARAMETERS OF THE SIMULATION SYSTEM

MMC converter	
Number of sub-modules per arm	216
Rated sub-module capacitor voltage	2.2kV
Sub-module capacitor	4.5mF
Inductance of arm inductor	15mH
Resistance of arm inductor	10mΩ
Controller sampling frequency	10kHz
Smoothing reactor	
Resistance	36mΩ
Inductance	10mH
HVDC transmission line	
Rated voltage	400kV
Rated current	1kA

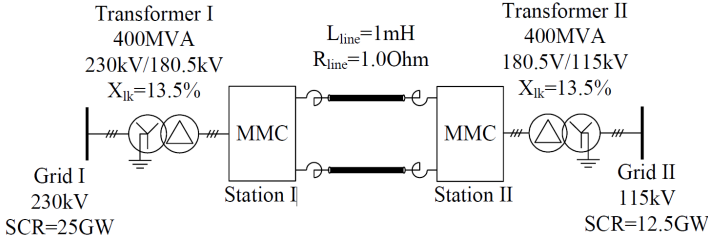


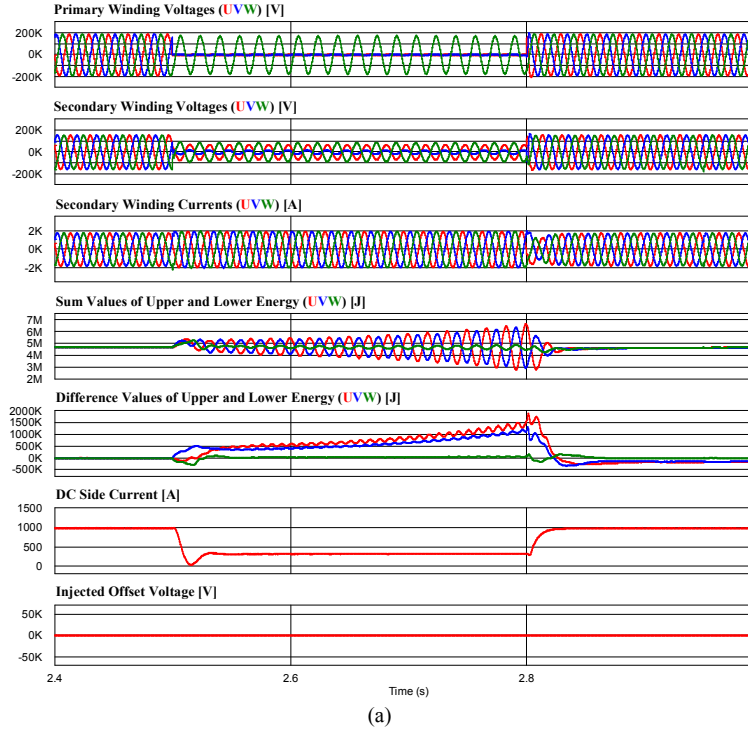
Fig. 8. Schematic of the simulated point-to-point MMC-HVDC system.

Fig. 9 shows the simulation results of station-I in Fig. 8 with the conventional and the proposed control method, respectively, during 0.3s of double line-to-ground (DLG)

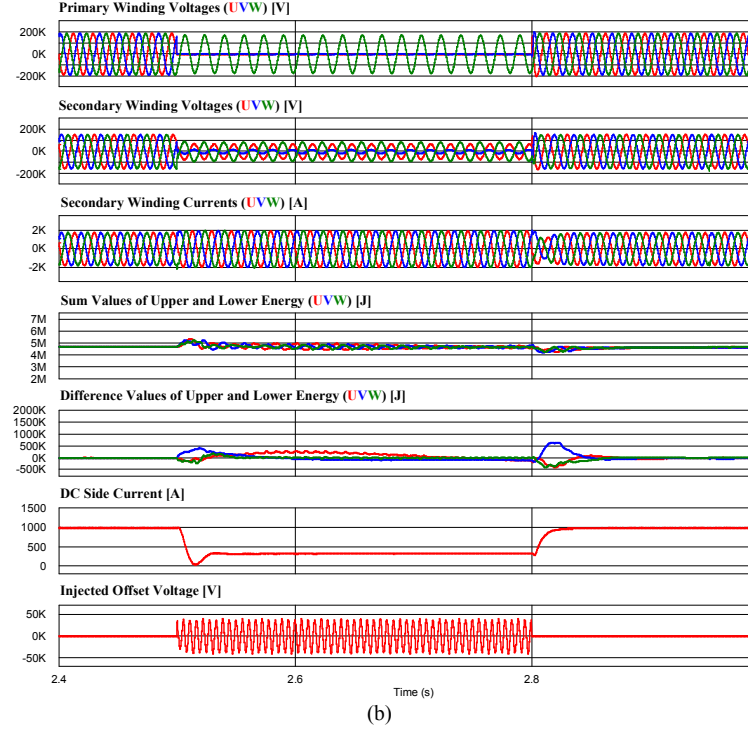
fault at Grid-I. At 2.5s, the AC transmission lines of u- and v-phases in grid side come into solid contact with the ground. In Fig. 9(a), if the conventional method in [9-10] is employed, the system balance starts to collapse. The energy differences of upper and lower arm at three phases which is the 5th trace of Fig. 9(a) are getting larger after DLG fault in the grid. At 2.8s, the energy difference at u-phase corresponds to about 0.7p.u. of the rated arm energy, 2.35MJ. If the real MMC system is faced on the same severe situation, the system would be shut down consequently. In the 4th trace in Fig. 9(a), sum values of upper and lower energy have small DC and large fundamental frequency component. The considerable magnitude of the circulating currents due to the diverged balancing controller results in the heavy fundamental frequency power and severe energy fluctuations at u- and v-phases appear during DLG fault. These results reveal that the conventional balancing method cannot be an option of fault ride through control method against severe DLG fault. However, when the proposed method is employed, the balancing control is kept despite the severe DLG fault conditions as shown like Fig. 9(b). After the fault is detected, the controller produces the offset voltage in the AC output voltages. As shown in the 7th trace of Fig. 9(b), the third harmonic frequency offset voltage is injected and the magnitude of injected voltage is set to be 30% of the pole voltage margin. However, the injected offset voltage causes the fluctuation of DC line voltage potential to earth ground, and it can have harmful effects on DC line isolations. Because the DC transmission line is usually designed to endure the pole-to-ground DC short fault, the DC transmission line has no problem about isolation margin by the injected offset voltage. The energy difference in the 5th trace of Fig. 9(b) is below the allowable bound and the energy sum in 4th trace is also well controlled with very small fluctuations. Therefore, the proposed method can be a promising option of fault ride through control method against DLG fault.

## VI. CONCLUSIONS

In this paper, a balancing control method for HVDC transmission system based on MMC has been proposed against double line grid fault. By the proposed control method, the system can keep its cell capacitor energy balancing capability even under the severe double line fault in AC grid, and the dynamics of cell voltage balancing under the fault have been improved conspicuously. The validity of the proposed method has been supported by the computer simulation results. In contrast to the conventional control strategy, the fault ride-through capability of the MMC-HVDC system could be much enhanced if the proposed method is incorporated in the cell voltage balancing controllers.



(a)



(b)

Fig. 9. Dynamic responses under a double line-to-ground fault at grid, (a): with the conventional control method, (b): with the proposed control method.

- [2] S. Allebrod, R. Hamerski, and R. Marquardt, "New transformerless, scalable modular multilevel converters for HVDC-transmission," in Proc. IEEE PESC, 2008, pp. 174-179.
- [3] B. Gemmell, J. Dorn, D. Retzmann, and D. Soerangr, "Prospects of multilevel VSC technologies for power transmission," in Conf. Rec. IEEE-TDCE, 2008, pp. 1-16.
- [4] A. Lesnicar and R. Marquardt, "An innovative modular multilevel converter topology suitable for a wide power range," in Proc. IEEE Boogna Power Tech, 2008, vol. 3, pp. 1-6.
- [5] D. Peftitsis, G. Tolstoy, A. Antonopoulos, J. Rabkowski, J. K. Lim, M. Bakowski, L. Angquist, and H. P. Nee, "High-power modular multilevel converters with SiC JFETs," in Proc. IEEE ECCE, 2010, pp. 2148-2155.
- [6] Rainer Marquardt, "Modular Multilevel Converter Topologies with DC-Short Circuit Current Limitation," in Proc. IEEE ECCE Asia, 2011, pp. 1425-1431.
- [7] N. hmed; L. Angquist, S. Norrga, H.-P. Nee, "Efficient modeling of modular multilevel converters in HVDC-grids under fault conditions," PES General Meeting | Conference & Exposition, 2014 IEEE , vol., no., pp.1,5, 27-31 July 2014.
- [8] Xiaofang Chen, Chengyong Zhao, Chungang Cao, "Research on the fault characteristics of HVDC based on modular multilevel converter," Electrical Power and Energy Conference (EPEC), 2011 IEEE , vol., no., pp.91,96, 3-5 Oct. 2011.
- [9] S. Cui, S. Kim, J.-J. Jung, and S.-K. Sul, "A Comprehensive Cell Capacitor Energy Control Strategy of a Modular Multilevel Converter (MMC) without a Stiff DC Bus Voltage Source," 2014 Applied Power Electronics Conference and Exposition, 2014-Mar., 2014.
- [10] J.-J. Jung, S. Cui, S. Kim, and S.-K. Sul, "A cell capacitor energy balancing control of Modular Multilevel Converter considering the unbalanced AC grid conditions," Power Electronics Conference (IPEC-Hiroshima 2014 - ECCE-ASIA), 2014 International, vol., no., pp.1268,1275, 18-21 May 2014.
- [11] Hong-Seok Song and Kwanghee Nam, "Dual current control scheme for PWM converter under unbalanced input voltage conditions," Industrial Electronics, IEEE Transactions on , vol.46, no.5, pp.953,959, Oct 1999.
- [12] Xiaojie Shi, Zhiqiang Wang, Bo Liu, Yiqi Liu, L. M. Tolbert, and F. Wang, "Characteristic Investigation and Control of a Modular Multilevel Converter-Based HVDC System Under Single-Line-to-Ground Fault Conditions," Power Electronics, IEEE Transactions on , vol.30, no.1, pp.408,421, Jan. 2015.
- [13] S. Cui, J.-J. Jung, Y. Lee, and S.-K. Sul, "A Novel Control Strategy of a Modular Multilevel Converter (MMC) based VSC-HVDC Transmission System," 2015 Applied Power Electronics Conference and Exposition, 2015-Mar., 2015.
- [14] Guan, Minyuan, and Zheng Xu, "Modeling and control of a modular multilevel converter-based HVDC system under unbalanced grid conditions," Power Electronics, IEEE Transactions on 27.12 (2012): 4858-4867.
- [15] Haitian Wang, Guangfu Tang, Zhiyuan He, Jie Yang, "Efficient Grounding for Modular Multilevel HVDC Converters (MMC) on the AC Side," Power Delivery, IEEE Transactions on , vol.29, no.3, pp.1262,1272, June 2014.

## REFERENCES

- [1] T. K. Vrana and O. Fosso, "Technical aspects of the North Sea super grid," CIGRE ELECTRA, no. 258, pp. 6-19, Oct. 2011.